Pure Appl. Chem., Vol. 78, No. 6, pp. 1239–1252, 2006.
doi:10.1351/pac200678061239

Metal halide lamps: Gravitational influence on color separation*

W. W. Stoffels[1,‡], A. J. Flikweert[1], T. Nimalasuriya[1], J. J. A. M. van der Mullen[1], G. M. W. Kroesen[1], and M. Haverlag[2]

[1]Eindhoven University of Technology, P.O. Box 513, 5600 MB Eindhoven, The Netherlands; [2]Central Development Lighting, Philips Lighting, P.O. Box 80020, 5600 JM Eindhoven, The Netherlands

Abstract: Metal halide lamps are very efficient light sources based on a Hg plasma arc with metal halide salt additions. In spite of their high efficiency, the lamps suffer from several problems, such as color separation and instabilities, which currently hinder large-scale use. These phenomena are caused by a complex interaction of convection and diffusion flows in the plasma. In order to unravel the various contributions, experiments under microgravity have been performed where convection is absent.

The experiments confirm the previously held qualitative views, but also provide absolute data on densities and temperatures that will be used to validate numerical models of these lamps.

Keywords: plasmas; lamps; metal halide; microgravity; high pressure; lighting.

INTRODUCTION

Looking at Earth from a distance, as shown in Fig. 1, it is not the Great Wall of China or any of the large cities that will first signify human activity. It is the billions of lights we use which light up nearly all parts of the night sky. Wherever humans are present, artificial light is used, allowing us to live and work indoors and outdoors at any time of the day. In densely populated areas, this literally lights up our planet. Light is certainly a great commodity, but it comes at a price. Not only does it result in serious light pollution, disturbing animal and plant life, it also has a huge energy need. Of the annual world electricity production of 15×10^{12} kWh, about 20 % is used for lighting applications [1,2]. Let us try to put this enormous number into perspective. A medium- to large-sized electricity plant has a production capacity of about one GW, which corresponds to about 8 10^9 kWh per year. So worldwide there are about 375 electricity plants operating continuously solely to supply the power for our lamps. Apart from depleting our fuel reserve, this also results in an annual emission of about 2×10^9 tons of CO_2, which is a significant contribution to global heating. These numbers shows that lighting has a large economical as well as ecological impact.

*Paper presented at the 17th International Symposium on Plasma Chemistry (ISPC 17), Toronto, Ontario, Canada, 7–12 August 2005. Other presentations are published in this issue, pp. 1093–1298.

‡Corresponding author

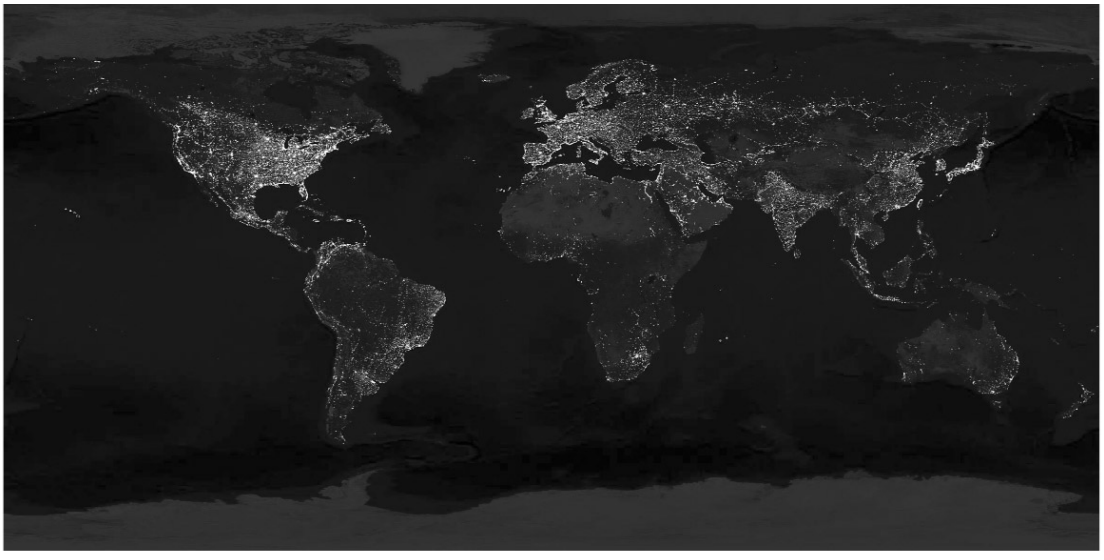

Fig. 1 A composite satellite view of the earth by night. The visible light is virtually all produced by discharge lamps. (Picture courtesy of: C. Mayhew and R. Simmon (NASA-GSFC), NOAA/NGDC, DMSP Digital Archive).

Thinking about lighting and lamps, the thing that first comes to mind is the incandescent lamp, see Fig. 2a. It has been around for about 150 years and is based on the well-known technology of electrically heating a tungsten wire, until it is hot enough to emit visible light. Most light is, however, produced by gas discharge lamps. These can be grouped into two large families: low-pressure lamps, with the tubular fluorescent lamps, commonly used in offices as the best-known example (Fig. 2b), and high-pressure lamps, commonly used if much light is needed (Fig. 2c).

It should be noted that apart from the incandescent and gas discharge lamps, solid-state lighting in the form of light-emitting diodes (LEDs) is gaining ground rapidly. In the coming years, many new applications based on LED technology are expected and they will take their place next to the two existing technologies. Currently, their market share in general lighting applications is still small, and it is expected to take several years and significant technical breakthroughs before they can seriously compete with the high-power plasma lamps.

Based on numbers of lamps sold, the average lifetime, and lamp efficiencies, some reasonable estimates can be made. Such an exercise shows that incandescent lamps consume 20 % of the power needed for lighting, while 80 % is used for plasma-based lamps. Taking into account the fact that plasma lamps are 5 to 10 times more efficient, this implies that about 97 % of all artificial light on Earth is produced using plasma technology [1,2]. Evidently, plasma lamps are essential in lighting, and any increase in their efficiency, even by as little as 1 %, has a large impact on preserving our natural resources and environment.

This contribution concentrates on the metal halide lamp. It is a high-pressure gas discharge lamp with a very high efficiency. Despite the fact that the lamp is commercially widely available in a great variety of forms and applications, there are still several technological and scientific problems, which limit its applicability. Some of the problems are related to a limited understanding of the fundamental processes within the gas discharge, and these are the focus of the current study. Below, we will explain the workings of a metal halide lamp, discuss some of its problems, and show experiments that reveal the workings of the lamp.

Fig. 2 Various lamp types (not to scale). Left: an incandescent lamp, typical size 5–10 cm. Right: a high-pressure lamp, with typical dimensions of centimeters. Bottom: a low-pressure fluorescent lamp, with a typical length of 1 m.

METAL HALIDE LAMPS

A metal halide lamp is derived from the well-known Hg high-pressure arc discharge [3]. A schematic picture is shown in Fig. 3. An electrical arc is maintained between two electrodes, which are sealed into the confining space of the lamp burner. In normal operation, the main gas in the lamp is Hg. Depending on lamp type, size, and application, the pressure varies from a few to several hundred bar. The center of the arc is 5000–6000 K, while the wall is maintained at 1000–1500 K. As the lamps are in the millimeter to centimeter size range, this implies that there are strong temperature gradients. Still, the lamp is assumed to be close to local thermodynamic equilibrium (LTE), especially in the central part of the lamp, where most light is generated. In order to facilitate igniting the lamp, a small amount of a noble gas like Ar or Kr is added. A high voltage peak starts the lamp in the noble gas, but after a few seconds the Hg starts evaporating, and, due to its lower ionization energy, the arc soon becomes a Hg discharge. Hg is a very efficient radiator, and Hg lamps are commonly used. The main Hg emission lines, however, are in the UV region. This implies that a fluorescent coating on the lamp is needed, which transforms a UV photon into a visible one. By mixing various coatings, a good color rendering of the lamp is obtained, very similar to the well-known low-pressure tubular fluorescence lamps (Fig. 2, bottom). As the energy of a visible photon is about half that of the UV photons, the Hg emission efficiency is only partly utilized. Metal halide lamps use the efficiency of a Hg discharge, while emitting directly visible photons, thus eliminating the need for fluorescent coatings. This is achieved by adding a mixture of rare earth halide salts (such as DyI_3, ScI_3, CsI_2, or NaI). Since the melting and boiling temperatures of these salts are high, they never fully evaporate, but equilibrium is established at the coldest spot in the lamp. Consequently, the salts are present in the form of unsaturated vapor in all hotter regions of the lamp. Obviously, in the hot central arc region, the salt will dissociate and the metals will be excited and ionized. Like Hg, these metals are efficient radiators, however, most light is emitted in the visible region. As a result, metal halide lamps can be made, with power efficiencies up to 40 %, significantly better than most other lamp types. A good color rendering is achieved by mixing various salts. Currently, these lamps are used for industrial lighting, street lighting, and city beautification. Unfortunately, the

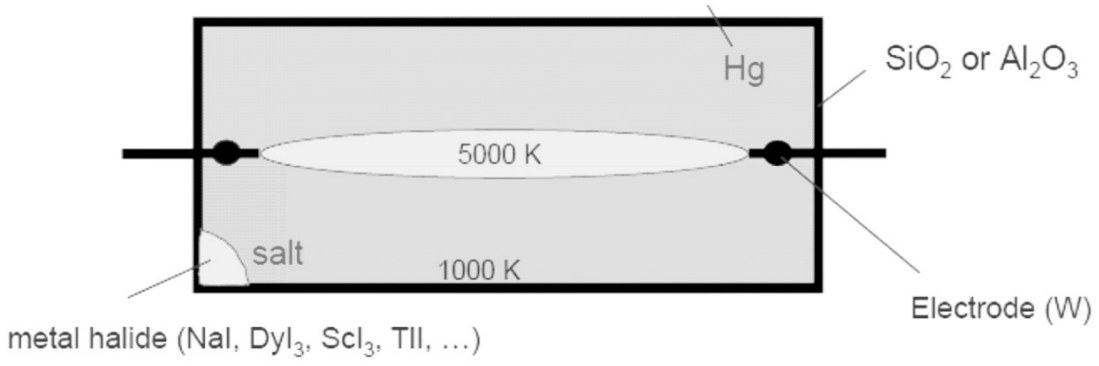

Fig. 3 A schematic view of a metal halide lamp. The arc is produced between to tungsten electrodes in a Hg buffer gas of about 10 bar. The arc is confined inside an SiO_2 or Al_2O_3 burner. Furthermore, a metal halide salt like NaI, DyI_3, ScI_3, or TlI is added. After evaporation and dissociation, the excited metal atom is the main radiation source.

lamp also suffers from several problems, which limits its use for other applications, such as shop and home lighting. These problems include electronic control of the lamp, burning orientation, instabilities, and (re-)ignition problems [4].

In this paper, we will focus on the problem of color separation in metal halide lamps. Before going into a detailed explanation of the effect and showing the experimental data, let us conclude the general description of a metal halide lamp with a remark on the Hg. As commonly known, Hg is unhealthy and thus Hg-free lamps are desirable. However, Hg lamps in general and metal halide lamps in particular are highly efficient. It should be noted that there are small amounts of Hg in the average fuel mix of electricity plants. During the long lifetime of these lamps, generally about five to ten times more Hg is released into the atmosphere by electricity plants supplying the lamp power, than is present in the lamp. Moreover, the Hg in these lamps is easily recyclable. Thus, by introducing a Hg-free lamp, a loss of lamp efficiency is not acceptable. For general lighting applications, there are currently no good alternatives for the Hg-containing lamps, thus it is important to understand how they work in order to further improve their performance.

COLOR SEPARATION IN METAL HALIDE LAMPS

In this paper, we will focus on the physical and chemical processes responsible for color separation in metal halide lamps. As mentioned before, the main emission from the lamps results from excited atomic and ionic metal species and lamp efficiency will generally increase if there is more metal in the central region.

If the wall temperature and the basic thermodynamic data of the salt or salt mixture are known, the vapor pressure of the metal salt above the solid salt can also be calculated. If the temperature distribution within the lamp is known, it is relatively easy to make an LTE approximation of the partial pressures of the various chemical compounds in which the metal exists at different places in the lamp. Figure 4a shows for DyI_3 how the LTE distribution of the partial pressures for the various species looks throughout the lamp. In the calculations, a Hg pressure of 10 bar is assumed and a constant partial elemental pressure is defined as the summed pressure of Dy^+, Dy, DyI, DyI_2, DyI_3, Dy_2I_6, and Dy_3I_9—with the latter two counting double, respectively triple. In equilibrium, the elemental pressure equals the saturated vapor pressure at the wall. A 4-mm-radius lamp having a parabolic temperature profile with a wall temperature of 1100 K and an axis temperature of 5500 K is assumed in order to plot the pressures as a function of lamp radius.

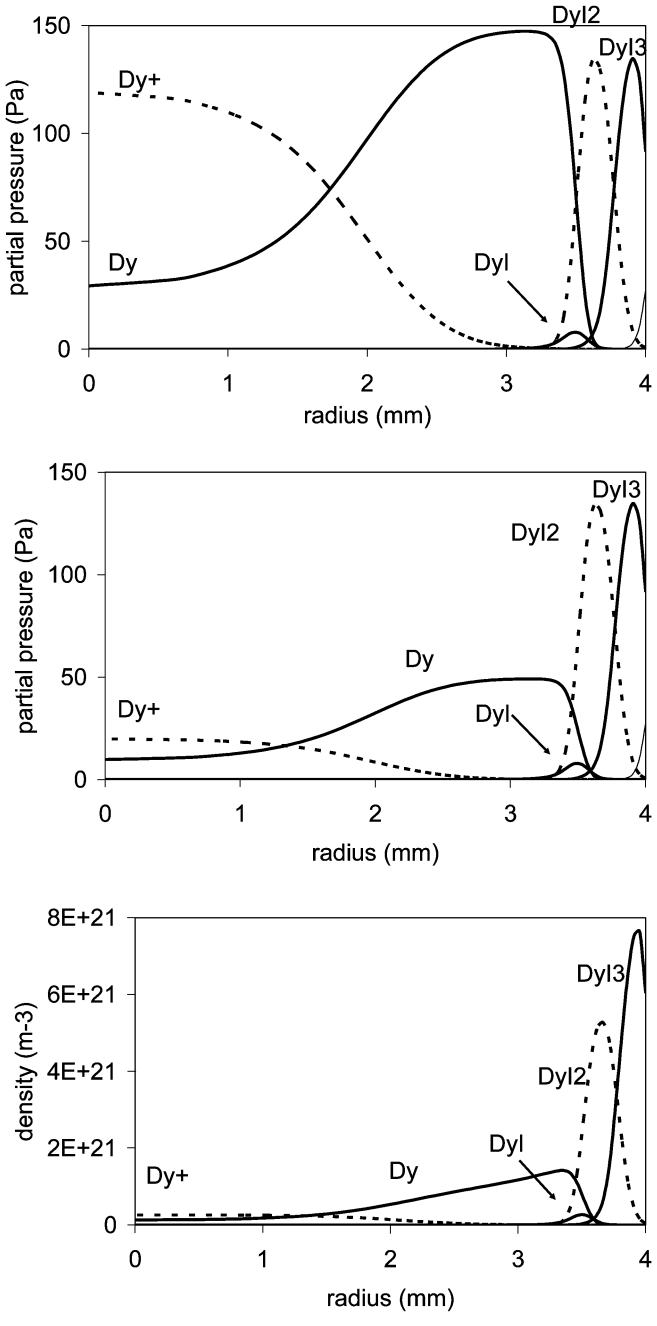

Fig. 4 DyI_y species under chemical LTE conditions as a function of lamp radius. A 10 bar Hg plasma and a parabolic temperature profile with an axis temperature of 5500 K and a wall temperature of 1100 K are assumed. (a) LTE calculations without transport. (b) LTE calculations, assuming a stationary state and taking into account the differences in diffusion coefficients between molecules atoms and ions. (c) Density of DyI_y species as a function of radius under the conditions of Fig. 4b. No convection (microgravity condition) is assumed for all calculations.

Figure 4a shows that in the center of the lamp, ions and atoms dominate, whereas close to the wall there are only molecules. The latter is fortunate as metallic atoms will react rapidly with the lamp wall, forming an undesired opaque chemically stable layer.

In spite of the imposed constant elemental pressure, the plasma-induced temperature gradient results in strong gradients of the individual species' pressures. This causes a strong diffusion flux of the species, which in steady state is counteracted by the back-diffusion of other species. In our case, however, the diffusion speed of the molecules will be significantly smaller than that of the atoms due to their size and mass difference. Ions and atoms have similar masses, but ions can diffuse faster due to ambipolar diffusion. In order to reach a stationary state, a gradient in the elemental pressure has to exist, such that the lower molecular diffusion speed is balanced by a higher pressure. Similarly, the ionic pressure is lower than the atomic pressure due to its enhanced ambipolar diffusion, as shown in Fig. 4b. The effect of a nonconstant elemental pressure as a function of lamp radius is called radial segregation. Light is emitted by individual atoms and ions, therefore, the density, defined by the ideal gas law, rather than the pressure is the controlling parameter. As the central temperature is higher than the wall, the density is lower. This further increases the difference between the wall and center of the plasma, see Fig. 4c. Also note that in a cylindrical type lamp, the lamp volume depends on the square of the radius, thus the region with the high salt density between 3 and 4 mm is roughly equally large as the central zone up to 3 mm. All these effects combine to a low amount of radiating species in the hot central zone, thus lowering the lamp efficiency.

In addition to the diffusion effects described above, there is also convection in the lamp. In a horizontally operating lamp, convection will counteract the diffusion as it effectively "mixes" the various lamp species as graphically depicted in Fig. 5. Unfortunately, in horizontally operating lamps, convection will lift the hot arc into the curved shape from which it derives its name. This brings the hot plasma region close to the cold wall, which at best lowers the lamp efficiency and in worse cases causes lamp failure. As a result, many high-pressure lamps are operated in a vertical orientation.

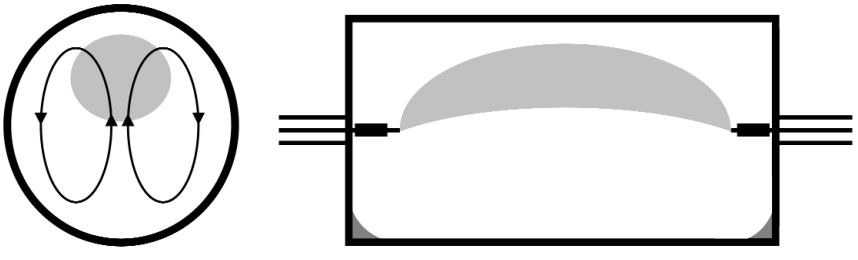

Fig. 5 Schematic drawing of the influence of convection and formation of a curved arc (grayed area) in a horizontally burning lamp. It results in an efficient mixing of species (shown left in a longitudinal view) but also in an undesired curved shape of the plasma arc (shown right in a sight-on view).

In vertically operating lamps, convection causes species in the hot central arc region to rise and to descend along the cooler walls [3]. The radially segregated minority salt species (Fig 4b) follow the dominant Hg flow. The combined effect of convection and radial segregation is an increased elemental metal density in the lower part of the lamp. Such axial segregation results in a nonhomogeneous emission over the lamp, called color separation. An example of this effect is shown in Fig. 6. A simple theory, based on infinitely long lamps predicts an exponential decay of the metal density as a function of height in the lamp [5,6]:

$$n(z) = n(0) \exp(-\lambda z) \quad (1)$$

where λ is called the segregation parameter.

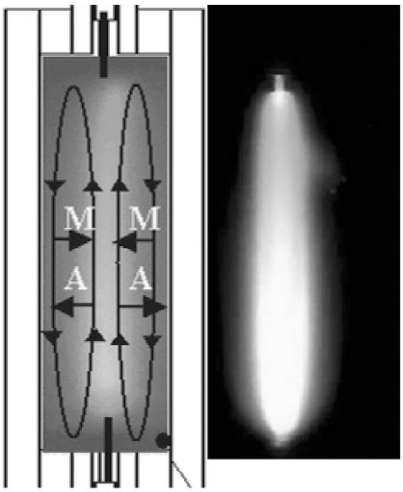

Fig. 6 Axial segregation and color separation in a vertically operating metal halide lamp due to the combined effects of diffusion and convection. (a) Artist's impression of the diffusion and convection flow. (b) Picture of a lamp with color separation.

The value of λ depends on the relative importance of convection versus diffusion. In the absence of convection, there is only radial and no axial segregation, so $\lambda = 0$. With increasing convection, axial segregation and color separation occur, thus λ increases. If convection becomes faster than diffusion, convective mixing of species occurs. This reduces the radial segregation, which in turn reduces the color separation. Thus, for very large convective flows, the convection parameter λ tends to zero again. Consequently, λ and thus color separation are expected to have a maximum when diffusion and convection processes are of equal magnitude and to be small in case of either weak or strong convective flows.

Qualitatively, this yields a good description of the high-intensity discharge (HID) lamp. In practical lamps, however, several other effects, such as electrodes, burner geometry, end effects, and specific chemistries, also affect the lamp behavior. In order to fully understand the lamp and to make quantitative predictions on light output, a numerical lamp model is under construction [7]. To provide input data and verify the model results, a large variety of experiments are necessary. From the previous discussion, it follows that convection plays a key role in understanding the lamp behavior.

This has been proven by observing the lamp behavior during a space shuttle flight [8]. To be able to unravel the complex interaction between convection and diffusion, extended experiments under zero gravity have been performed. Convection is eliminated in the absence of gravity, so the effect of diffusion only can be studied and compared with the model results. Two microgravity experiments have been performed, the first during parabolic free falls in an air plane and the second in the international space station (ISS).

REFERENCE LAMPS

The lamps are studied using various diagnostics. Obviously, it should be possible to compare experimental results; moreover, the experimental data need to be compared with numerical models. Therefore, a reference lamp has been defined that can be readily experimentally diagnosed as well as numerically modeled. This lamp, described below, is now in use by several research groups working on metal halide lamps. Several demands have been incorporated into the design. To be accessible by optical techniques, quartz has been chosen as the wall material. To simplify modeling, the burner is cylindrically shaped

with a 4-mm inner radius and 20 mm in length. The lamp is placed in an outer tube with symmetric double-ended electrical connections and standard electrodes with an inter-electrode distance of 18 mm. In the experiments described here, the outer tube is under vacuum, preventing heat losses. It also can be filled with nitrogen, which prolongs the lamp lifetime. To simplify the lamp chemistry, only a single relatively well-known metal halide salt is added: DyI_3. Hg is the buffer gas, and an Ar/Kr mixture is used as a starting gas. The lamp power is moderated to about 100 W.

A picture of the lamp is shown in Fig. 7. Detailed optical emission measurements have been performed on the lamp [9]. Place-resolved Bolzmann plots have been constructed, similar to the example shown in Fig. 8, which show that the center of the plasma arc is close to LTE with a temperature of about 5500 K and an electron density in the order of 10^{21} m^{-3}. In spite of uncertainties in transition probabilities [10,11], serious deviations from LTE have been found near the plasma edge. These are probably due to large radiative energy losses: this plasma is after all meant to be a lamp. Diode laser absorption spectroscopy [12] has been used to probe the Dy ground-state density. The results, depicted in Fig. 9, show that there is significant axial segregation of the Dy in the lamp. Apart from electrode effects, the segregation is well described by the exponential decay formula given by eq. 1.

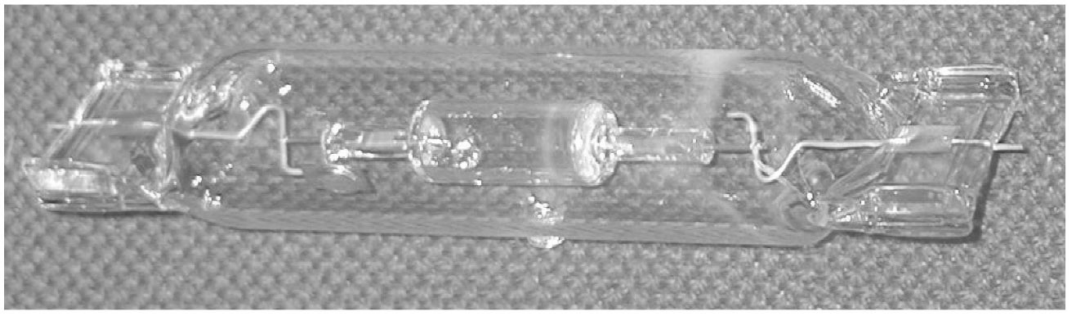

Fig. 7 Picture of the reference metal halide lamp. The inner burner (4 mm radius, 20 mm length) is positioned inside the outer tube are by the wires connecting the electrodes. The yellowish deposition on the right-hand side of the burner is the DyI_3 salt.

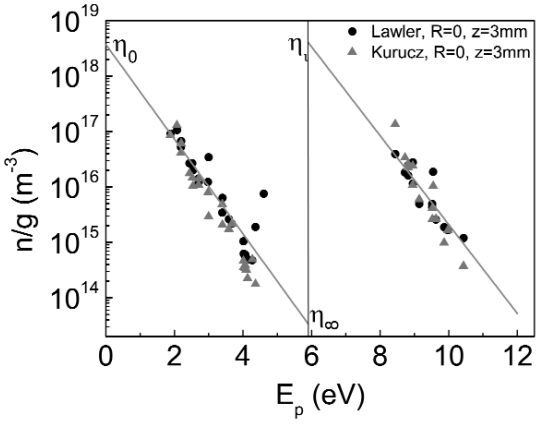

Fig. 8 Boltzmann plot of various atomic and ionic Dy levels, obtained by Abel inversion of radially resolved absolute line intensity measurements [9]. The data are obtained in the center of a standard lamp with 10 mg Hg 3 mm above the lower electrode using a lamp power of 100 W. The dots and triangles represent the same measurements, but using different atomic transition probabilities to determine the absolute state density: dots [10], respectively, triangles [11].

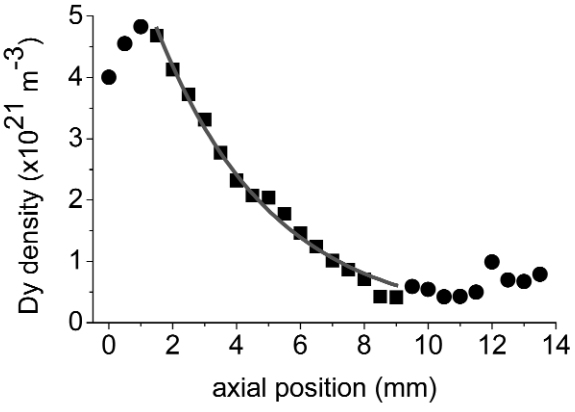

Fig. 9 The atomic Dy density measured by diode laser absorption spectroscopy as a function of height above the lower electrode in a lamp with 10 mg Hg at 113 W lamp power. The exponential segregation fit (eq. 1; λ = 0.28/mm) is only applied to the square dots [12].

MICROGRAVITY MEASUREMENTS

The experiments have been performed in an Airbus during 34th, 35th, and 37th parabolic flight campaigns of the European Space Agency (ESA) in 2003 and 2004 and during the Delta Soyuz mission in the ISS in April 2004. During a parabolic flight, a level-flying airplane pulls up strongly before closing the engines and going into a parabolic free fall for about 20 s. At the end of the parabola, a second strong acceleration is used to prevent the plane from crashing. The result is that the experiments inside the plane are subjected to a series of 1–1.8–0–1.8–1 g gravity conditions. During the hypergravity (1.8 g) phases, there is an increased convection, whereas there is no convection during the microgravity phase.

Four different diagnostics have been used during parabolic flights: optical emission and laser absorption spectroscopy, a video camera, and a light-integrating sphere. Since the optical emission set-up was a prototype of the version in the ISS, it had to be small, light-weighted, and compact. The requirement for compactness is solved by using an Echelle-type grating with a high blaze angle (74°). Because of the high dispersion, due to the high angle of incidence and the high orders used, the focal length of the main lens can be relatively small, and consequently the spectrometer can be very compact, about 20 cm in length. A disadvantage of Echelle-type spectrometers is their small free spectral range (FSR), which results in wavelength overlapping of adjacent orders. By installing an interference filter in the optical system selecting a small wavelength interval, the problem of overlapping orders is avoided. In our set-up, several interference filters can be selected, providing wavelength selection. Consequently, the angle of the grating can remain fixed. This provides a very small but robust set-up with a similar resolution and spectral range as the 1-m monochromator used in the laboratory (cf. Fig. 8 [9]). The set-up allows us to reconstruct a radially resolved atomic-state density distribution function and a radial temperature profile during microgravity. The diode laser absorption system is essentially a copy of the laboratory system (cf. Fig. 9 [12]) measuring the Dy ground-state density. Video images provided by a stripped webcam are used to monitor the experiment and get qualitative information on the lamp behavior. All hardware is integrated on one frame, which is enclosed by an aluminum dome structure. The frame holds the spectrometer, the video camera, and the diode laser absorption set-up. It also supports the rotating lamp holder in which 20 lamps can be mounted.

During the parabolic flights, an additional set-up has been used with a spectroscopically integrating sphere (Fig. 10) to measure the total light output under varying gravitational conditions [13]. The light is detected by a photodiode supplied with a suitable optical filter, simulating human eye sensitivity. Thus, the lamp efficacy and power efficiency can be determined.

Fig. 10 Picture of the inside of an integrating sphere. The lamp is mounted in the middle. Light is reflected diffusely multiple times by the white reflective coating of the sphere before it is detected by a small detector in the wall supplied with a suitable optical filter. Thus, the detector signal corresponds with the integrated lamp efficacy.

Due to increased weight and size limitations, the laser absorption part of the set-up was not incorporated in the ISS version of the experiment, reducing it to less than 30 kg.

Figure 11 shows the ISS flight hardware, just before the aluminum safety dome is mounted on the bottom plate which holds the frame. The astronaut, André Kuipers, operates the experiment using a human–machine interface. The ISS experiments have been performed in the ESA Microgravity Science Glovebox, in the U.S. Destiny lab during the Delta Soyuz mission in April 2004.

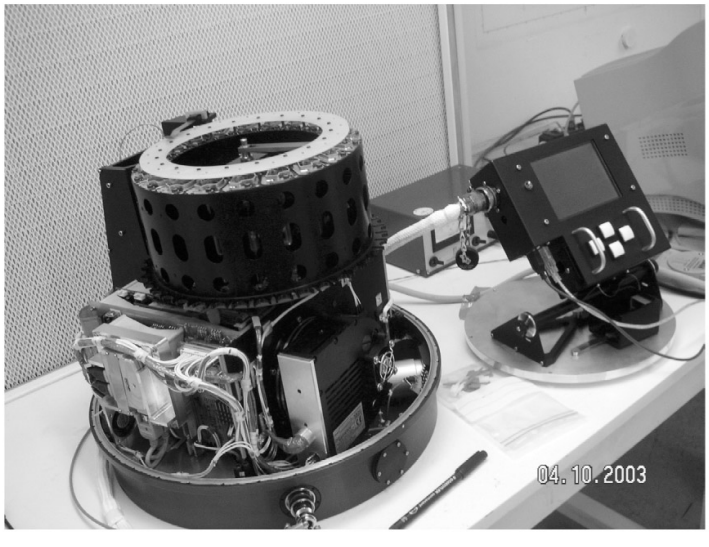

Fig. 11 Picture of the inside of the experiment used in the ISS. The top part is a carousel with 20 lamps, while the lower part contains the power supply and emission spectroscopy diagnostics. A protective aluminum dome (not shown), covering the set-up is mounted before launch. The astronaut cannot reach the experiment directly, but operates through the human–machine interface, shown on the right.

Figure 12 shows pictures of the lamp during various phases of the parabolic flight. The color separation is clearly visible, as the lower part of the lamp emits bright white light, whereas in the top part only a weak Hg emission is seen. The segregation in the hypergravity phase is significantly less than under normal gravity conditions. In the microgravity phase, the light emission is homogeneous in the axial direction. Increased emission during hypergravity is confirmed by measurements with the integrating sphere (Fig. 13) [13]. The emission increase during the hypergravity phases shows that in this particular lamp, convection is already dominant during normal gravity. As a consequence, increasing gravity and therefore increasing convection leads to a better mixing and thus an increased light emission during the hypergravity phase. In the microgravity phase, convection is absent and radial segregation is dominant. In Fig. 13, this is clearly visible as a decrease in the emission, even below the 1 g value, at the start of the microgravity phase. The subsequent increase is caused by an increase of the lamp temperature in the absence of convective cooling. This results in a higher metal vapor pressure inside the lamp and thus a higher emission. It also shows that the 20 s of microgravity, available in an airplane, are insufficient to obtain a stable lamp. In order to study a fully stabilized lamp under microgravity conditions, measurements in the ISS are the only option. The more detailed optical emission and laser absorption data confirm the general trends observed with the webcam and integrating sphere (Figs. 12 and 13) and will be used to validate the lamp model. Preliminary data analysis shows that the radially resolved emission profiles can significantly change with varying gravity conditions [14]. Figure 14 shows the Abel inverted symmetrized emission profiles of excited atomic Dy (642.73 nm) in a lamp with 5 mg Hg during hyper- and microgravity. During the hypergravity phase, there is a reasonably homogeneous distribution of Dy, while under microgravity, radial segregation is so strong that it results in a nearly full depletion of the central region. As explained before, this is undesirable for an efficient lamp, but it also shows that these experiments help to unravel the complex transport processes in the lamp into their various parts. Figure 15 shows the image of the lamp during operation in the ISS. Under these conditions, there is no axial segregation and the lamp is completely homogeneous. Analysis of the data is underway, but preliminary data show a strong radial segregation of dysprosium, which allows for a strong Hg emission in the central region of the lamp, similar to the results shown in Fig. 14.

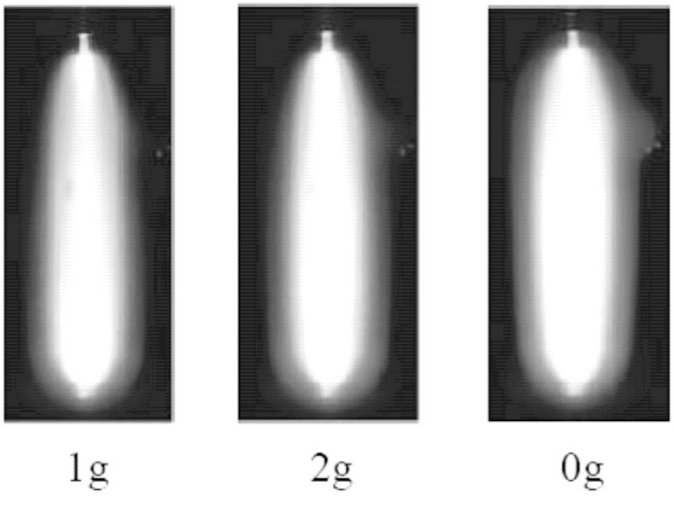

Fig. 12 Pictures of the lamp during normal gravity, hypergravity, and microgravity. The differences in the emission profiles are caused by a change in the Dy distribution inside the lamp due to varying convection and diffusion flows.

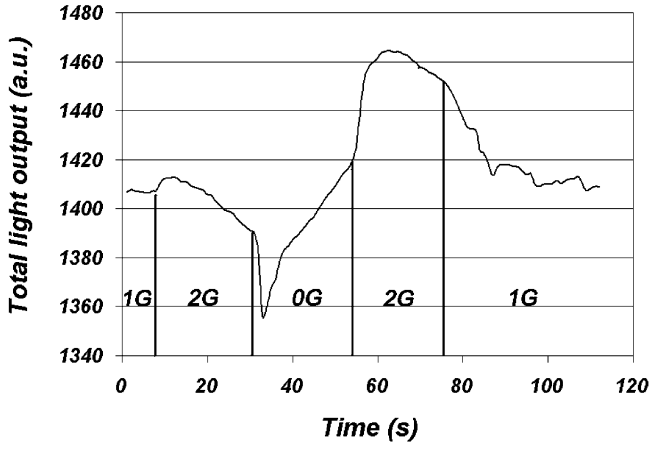

Fig. 13 Integrated light output of a 10-mg Hg lamp with DyI_3 (cf. Fig. 12) during a single parabola, measured using the integrated sphere shown in Fig. 10.

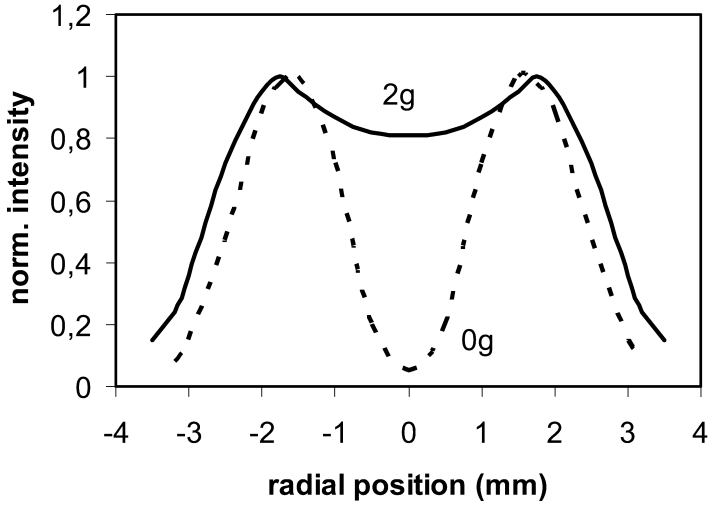

Fig. 14 Symmetrized and normalized radially resolved emission profiles of Dy during hypergravity (full line) and microgravity (dashed line) of a lamp at 90 W with 5 mg Hg [14].

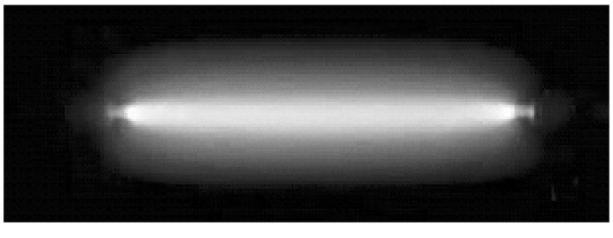

Fig. 15 Picture of the lamp during experiments in the ISS. As expected, the lamp emission is homogeneous in the axial direction.

CONCLUSIONS

Metal halide discharges are very efficient lamps. In spite of their advantages, there are still several issues limiting a wider applicability. One of the discharge-related problems is color separation, which is caused by a complex interaction of diffusion and convection transport of the light-emitting metal species in the discharge. It is currently beyond our capabilities to understand and model a general metal halide lamp with a complex shape and chemistry. Therefore, a simple reference lamp has been defined as useful for experiments and modeling.

To eliminate convection, experiments under microgravity have been performed during parabolic flights and in the ISS. Due to stringent weight, volume, and safety regulations, dedicated experimental designs needed to be developed, which proved to work successfully in the space station. The results support the qualitative theory of the lamp, but more importantly supply ample data for future model validation.

ACKNOWLEDGMENTS

This research is sponsored by the Space Research Organisation Netherlands (SRON), the Eindhoven University of Technology, Philips Lighting, the Netherlands Ministries for Education and Research and for Economic Affairs, Senter-Novem, COST, and STW. We acknowledge the support of ESA for the participation in the 34th, 35th, and 37th ESA parabolic Flight Campaigns and the Delta Soyuz mission. Particular thanks to astronaut André Kuipers, who performed the ISS measurements, the PLASIMO-team, and students M. Bax, D. van den Akker, G. Schiffelers, P. Kemps, F. van den Hout, and J. Beckers.

REFERENCES

1. The International Energy Association <www.iea.org> and the International Association for Energy Efficient Lighting <www.iaeel.org>.
2. M. Haverlag. "Een wereld verlicht door gasontladingen", inaugural speech, 10 June 2005, Eindhoven University of Technology, Netherlands (2005); digital form: <www.tue.nl/bib>.
3. W. Elenbaas. *The High Pressure Mercury Vapor Discharge*, North Holland, Amsterdam (1951).
4. (a) A. Lamouri, A. Naruka, J. Sulcs, C. V. Varanasi, T. R. Brumleve. *J. Phys. D: Appl. Phys*. **38**, 3028 (2005); (b) T. G. M. M. Kappen. *J. Phys. D: Appl. Phys*. **38**, 3033 (2005); (c) W. van Erk, J. Tu, J. Suijker. *J. Phys. D: Appl. Phys*. **38**, 3040 (2005); (d) Z. Tóth, Z. Koltai, G. Steinbach, A. Juhász, K. Váradi. *J. Phys. D: Appl. Phys*. **38**, 3047 (2005); (e) G. C. Wei. *J. Phys. D: Appl. Phys*. **38**, 3057 (2005); (f) B. J. de Maagt, A. Corazza. *J. Phys. D: Appl. Phys*. **38**, 3066 (2005); (g) J. E. Lawler, A. Koerber, U. Weichmann. *J. Phys. D: Appl. Phys*. **38**, 3071 (2005); (h) J. J. Curry, C. J. Sansonetti, J. Wang. *J. Phys. D: Appl. Phys*. **38**, 3086 (2005); (i) T. D. Dreeben. *J. Phys. D: Appl. Phys*. **38**, 3093 (2005); (j) P. Flesch, M. Neiger. *J. Phys. D: Appl. Phys*. **38**, 3098 (2005); (k) S. Lichtenberg, L. Dabringhausen, O. Langenscheidt, J. Mentel. *J. Phys. D: Appl. Phys*. **38**, 3112 (2005); (l) L. Dabringhausen, O. Langenscheidt, S. Lichtenberg, M. Redwitz, J. Mentel. *J. Phys. D: Appl. Phys*. **38**, 3128 (2005); (m) M. Redwitz, O. Langenscheidt, J. Mentel. *J. Phys. D: Appl. Phys*. **38**, 3143 (2005); (n) M. S. Benilov, M. D. Cunha, G. V. Naidis. *J. Phys. D: Appl. Phys*. **38**, 3155 (2005); (o) G. M. J. F. Luijks, S. Nijdam, H. van Esveld. *J. Phys. D: Appl. Phys*. **38**, 3163 (2005); (p) M. Weiß, H. Schubert, S. Meier, M. Born, D. Reiter, M. Strösser. *J. Phys. D: Appl. Phys*. **38**, 3170 (2005); (q) M. Kettlitz, M. Sieg, H. Schneidenbach, H. Hess. *J. Phys. D: Appl. Phys*. **38**, 3175 (2005).
5. E. Fisher. *J. Appl. Phys.* **47**, 2954 (1976).
6. H. P. Stormberg, *J. Appl. Phys*. **52**, 3233 (1981).

7. A. Hartgers, H. W. P. van der Heijden, M. L. Beks, J. van Dijk, J. J. A. M. van der Mullen. *J. Phys. D: Appl. Phys*. **38**, 3422 (2005).
8. A. H. Bellows, A. E. Feuersanger, G. L. Rogoff, H. L. Rothwell. *Study of Convection-free Metal Halide Lamps: Final Report on a Space Shuttle Experiment*, GTE Laboratories report: R&D/Tr85-038.1 (1985).
9. T. Nimalasuriya, A. J. Flikweert, W. W. Stoffels, M. Haverlag, J. A. M. van der Mullen, N. B. M. Pupat. *J. Appl. Phys.* **99**, 053302 (2006).
10. M. W. Wickliffe, J. E. Lawler. *J. Quant. Spectrosc. Radiat. Transfer* **66**, 363 (2000).
11. R. L. Kurucz, B. Bell. *Atomic Line Data*, Kurucz CD-Rom **23**, Smithsonian Astrophysical Observatory, Cambridge, MA (1993).
12. A. J. Flikweert, T. Nimalasuriya, C. H. J. M. Groothuis, G. M. W. Kroesen, W. W. Stoffels. *J. Appl. Phys*. **98**, 073301 (2005).
13. W. W. Stoffels, P. C. M. Kemps, J. Beckers, G. M. W. Kroesen, M. Haverlag. *Appl. Phys. Lett.* **87**, 241501 (2005).
14. G. Schiffelers. M.Sc. thesis, Eindhoven University of Technology (2003).